PERGAMON

Journal of Atmospheric and Solar-Terrestrial Physics 62 (2000) 527–540

Journal of ATMOSPHERIC AND SOLAR-TERRESTRIAL PHYSICS

Mapping of ionospheric outflows into the magnetosphere for varying IMF conditions

R.M. Winglee

Geophysics Program, University of Washington, Seattle WA 98195-1650, USA

Received 9 July 1999; received in revised form 24 September 1999; accepted 24 September 1999

Abstract

The presence of different ion species and components provides important insight into the processes that determine the entry, transport and acceleration of plasma within the magnetosphere. Multi-fluid simulations that include both ionospheric H^+ and O^+ and solar wind H^+ are used to evaluate the ionospheric outflows in response to a range of solar wind conditions. O^+ is particularly important as its provides a definitive means for determining the influence of ionospheric ions in the magnetosphere. While O^+ is gravitationally bound to the earth during quiet periods, enhancements in the cross-polar cap potential during southward IMF can produce centrifugal acceleration of the O^+ to produce enhanced outflows. However the same strong convective electric field causes much of this O^+ to be confined to the inner magnetosphere. During subsequent northward turning of the IMF, this ionospheric-rich plasma is ejected down the length of the deep tail. The derived O^+ density for this combination of alternate southward and northward IMF produces concentrations similar to those observed by Geotail.

1. Introduction

The magnetosphere is supported by plasmas from two sources: (1) the ionosphere, and (2) the solar wind. The presence of these populations in the magnetosphere can be inferred from the energy characteristics of the particle populations or by the presence of specific ion species. For example significant components of He^+ or O^+ would be suggestive of a strong ionospheric source whereas a strong solar wind component would be associated with significant components of He^{2+}. Understanding the presence of these different species provides important clues as to the processes governing the entry of plasma into the magnetosphere and the heating and acceleration of this plasma during disturbed periods.

Intense ionospheric outflows have been observed for more than two decades by polar orbiting spacecraft. Some of the earliest evidence for such strong outflows was provided by Shelley et al. (1972) who showed that during a magnetic storm the precipitating flux of keV O^+ ions could exceed that of H^+. Ionospheric outflows has since been documented by a variety of spacecraft, including ISIS-1 and -2 (Klumpar, 1979), S3-3 (Sharp et al., 1977; Ghielmetti et al., 1978; Gorney et al., 1981), DE-1 (Waite, 1985; Yau et al., 1985, 1988; Moore et al., 1986; Collin et al., 1987; Roberts et al., 1987; Pollock et al., 1990) and Akebono (Yau et al., 1993). Recent reviews of the importance of the ionospheric source are given by Yau and André (1997) and André and Yau (1997).

The calculated ion outflow led Chappell et al. (1987) to propose that the ionosphere was a sufficient source to populate the plasma sheet. This hypothesis lead Moore (1991) and Moore and Delcourt (1995) to propose that within the magnetosphere there was a

1364-6826/00/$ - see front matter
PII: S1364-6826(00)00015-8

boundary called the geopause, where the dynamics within this boundary were dominated by ionospheric plasma, and regions outside by plasma of solar wind origin. The geopause was envisaged to extend into at least the mid-tail region as suggested by single particle tracking (Delcourt et al., 1989; Delcourt et al., 1993).

More recently, Geotail observations have shown the presence of O^+ in both the mid-tail lobe/mantle (Mukai et al., 1994) and in the distant tail (Hirahara et al., 1996; Seki et al., 1996). A statistical study by Seki et al. (1998) showed that the lobe/mantle O^+ beams between 8 and 210 R_e have an average density during solar minimum of about 1×10^{-3} cm^{-3} which corresponds to about 1.2% of the proton component. In addition, the oxygen ions appear to have been strongly energized attaining energies up to about 3.5 keV.

However, there is equally compelling evidence that plasma of solar wind origin is also playing an important role in supplying plasma to the magnetosphere. Lennartsson (1987; 1992), has shown from ISEE 1 data that the plasma sheet always has a significant population of He^{2+} ions (indicating a non-negligible contribution from the solar wind source). This population was observed to be the largest during periods of extremely weak geomagnetic activity when the interplanetary magnetic field (IMF) was persistently northward. Recent Geotail observations also indicate the presence of a cold-dense stagnant ion component that is of magnetosheath origin and exists several R_E inside of the nominal position of the magnetopause (Fujimoto et al., 1998a, 1998b). Observations during a Wind perigee pass also show the presence of this cold-dense component in the plasma sheet and that mixing of ionospheric and solar wind plasma occurs across a wide section of the magnetotail (Li et al., 1999).

The very strong entry of solar wind plasma has been further documented in recent statistical studies between solar wind density observations and tail density measurements by Geotail (Terasawa et al., 1997) and by ISEE (Borovsky et al., 1997). In these studies, the density of the plasma sheet was shown to be proportional to that in the solar wind, particularly for northward IMF. This result is surprising in the sense that the magnetosphere is expected to be closed for northward IMF and open for southward IMF.

In order to understand the origins of the different plasma populations within the magnetosphere, a multi-fluid treatment of the magnetosphere was developed by Winglee (1998a, 1998b). Unlike MHD which is a single fluid treatment, the new method is able to distinguish the ionospheric populations from the solar wind populations, and provides the first 3D visualization of the geopause as a function of the solar wind conditions. These simulations allowed the concept of the geopause to be refined to include both the density and pressure geopauses where the contributions from the ionosphere and solar wind sources make equal contributions to the plasma density and pressure, respectively. Differences in the position of the density and pressure geopauses can provide important insight for example into the structure of the magnetotail including the merging of the low latitude boundary layer (LLBL) with the hotter plasma sheet.

These initial multi-fluid simulations were limited to treating only a plasma in which all the ions were H^+ and the identification of the different sources relied on the different energy characteristics of the particle distributions. In this paper the multi-fluid simulations are extended to include both H^+ and O^+ components so that the role of the ionospheric source can be directly identified through ion species measurements. In being able to account for the O^+, we are also then able to indirectly confirm the size of the geopause and the relative importance of the ionosphere in producing mass loading of the magnetosphere.

The simulation model is augmented with respect to previous models in that it not only includes different ion species but also includes gravity. This feature is important because much of the O^+ is expected to be gravitationally bound to the earth during quiet periods and some additional process is needed to accelerate the oxygen into the magnetosphere.

The model assumes a fixed oxygen concentration at the lower boundary of the simulations in order to evaluate changes in the ionospheric outflow driven solely by the solar wind conditions. In this limit the oxygen outflows are controlled by primarily two processes. The first is centrifugal acceleration (Cladis, 1986; Horwitz, 1987) where fast convection of magnetic field lines across the polar cap can produce sufficient velocities in the O^+ ions to overcome the gravitational force. The second process is through the buildup of large pressure gradients. This process is also convection related since enhancements in the cross-polar cap potential convect and compress the plasma to produce increased temperatures and densities in the inner magnetosphere. Such pressure excesses are seen in global models when there is a subsequent reduction in the cross-polar cap potential associated with changes in the solar wind conditions. These pressure excesses can drive plasma outflows into the deep tail.

In reality, the outflow of ionospheric ions is also controlled by a variety of processes that lead to the parallel acceleration of ionospheric ions out of the auroral zone (e.g., see the review by André and Yau, 1997). For example, various wave-particle interactions can produce large enhancements in the O^+ outflow at low altitudes. Some of these interactions appear to depend on auroral and solar activity. These interactions include heating by electrostatic and electromagnetic ion-cyclotron waves

(e.g., Singh and Schunk, 1985; Chang et al., 1986), and ion-ion two stream instability (e.g., Winglee et al., 1989). In addition, changes in the photoelectrons in the polar wind can produce changes in O^+ outflow of the order of 2–5 between solar minimum and solar maximum (Su et al., 1998). Thus, the model results presented here describe only the changes in ionospheric outflow driven by changes in the solar wind conditions and additional multipliers for the outflow need to be applied if the feedback on ionospheric conditions at low altitudes is to be included. The actual inclusion of these multipliers is beyond the scope of the present work since they are not well known at this time.

The model results show that for northward IMF only weak O^+ outflows are present and they are confined to primarily the lobe and plasmasphere. Because of the relatively weak convective electric field very little of the O^+ reaches the plasma sheet in the mid-tail region. As the average IMF is made increasingly more southward stronger O^+ outflows into the magnetosphere are driven by the enhanced centrifugal acceleration that accompanies the increase in convection of field lines over the polar cap, i.e. with increases in the cross-polar cap potential (see Section 3).

However, because the convective electric field is increasing in the tail at the same time, most of this O^+ is confined to the inner magnetosphere. Thus even for sustained southward IMF conditions, O^+ is not able to easily populate the mid- to deep-tail plasma sheet, and it appears that the strongest O^+ loading occurs for weak average IMF assuming steady-state solar wind conditions.

However, transients such as those that drive substorms can produce enhanced O^+ outflows into the deep tail well beyond those seen in the steady-state examples (see Section 4). The stronger flows arise from a two-step process. In the first step, there is enhanced storage of O^+ in the inner magnetosphere in association with growth phrase processes driven by sustained southward IMF which produces enhanced centrifugal acceleration over the polar cap and auroral regions. In the second step, with the turning of the IMF northward and the accompanying substorm onset, the cross-polar cap potential decreases and the plasma in the inner magnetosphere can no longer be confined and is instead ejected down the tail. O^+ outflows produced through this sequence lead to O^+ concentrations similar to the observations of Seki et al. (1996, 1998).

One consequence of this pumping action is that O^+ might not have a strong role in the initiation of onset of an isolated substorm, except possibly in the inner magnetosphere. However, during disturbed periods O^+ could possibly be a significant fraction of the plasma and thereby modify subsequent activity, including magnetic reconnection.

2. Multi-fluid simulations

An understanding of the influence of the different plasma components in the dynamics of the magnetosphere can be attained through the use of global multi-fluid simulations that track separately the interaction of the different fluids. The model used here is that same as used by Winglee (1998a, 1998b) used to identify the position of the geopause, except that it includes gravity and the model has been expanded to include three ion species (solar wind H^+, ionospheric H^+ and O^+, with one electron species which provides quasi-neutrality, and gravity. The dynamics of each component is given by

$$\frac{\partial \rho_\alpha}{\partial t} + \nabla(\rho_\alpha \mathbf{V}_\alpha) = 0 \tag{1}$$

$$\rho_\alpha \frac{d\mathbf{V}_\alpha}{dt} = q_\alpha n_\alpha \left(\mathbf{E} + \frac{\mathbf{V}_\alpha \times \mathbf{B}}{c}\right) - \nabla P_\alpha - \frac{GM_E \rho_\alpha}{R^2}\mathbf{r} \tag{2}$$

$$\frac{\partial P_\alpha}{\partial t} = -\gamma \nabla(P_\alpha \mathbf{V}_\alpha) + (\gamma - 1)\mathbf{V}_\alpha \nabla P_\alpha \tag{3}$$

where γ is the polytropic index, α denotes the different species, R is the radial distance, $\mathbf{r}$ is the unit vector in the radial direction, G is the gravitational constant and M_E is the mass of the earth.

These equations have to be simplified in order to attain a computationally feasible solution for global scale lengths. For the electrons, it is assumed that they have high mobility along the field lines and that the gravitational term for the electrons is much smaller than the other terms in the force equation. For these assumptions, the electrons can be assumed to be approximately in steady state or drift motion ($d\mathbf{V}/dt = 0$), so that the electron momentum equation reduces to

$$\mathbf{E} + \frac{\mathbf{V}_e \times \mathbf{B}}{c} + \frac{\nabla P_e}{e n_e} = 0 \tag{4}$$

Eq. (4) is equivalent to the modified Ohm's law with Hall and grad P corrections included. The rest of the electron dynamics are given by assuming quasi-neutrality, and applying the definitions for current, and electron pressure, i.e.,

$$n_e = \sum_i n_i, \quad \mathbf{V}_e = \sum_i \frac{n_i}{n_e}\mathbf{V}_i - \frac{\mathbf{J}}{e n_e}, \quad \mathbf{J} = \frac{c}{4\pi}\nabla \times \mathbf{B} \tag{5}$$

$$\frac{\partial P_e}{\partial t} = -\gamma\nabla(P_e\mathbf{V}_e) + (\gamma-1)\mathbf{V}_e\nabla P_e \tag{6}$$

The ion dynamics in the absence of gravity are attained by substituting the modified Ohm's law Eq. (4) for the electric field in the ion momentum equation, which gives

$$\rho_\alpha\frac{dV_{\parallel\alpha}}{dt} = -(\nabla P_\alpha)_\parallel - \frac{n_\alpha}{n_e}(\nabla P_e)_\parallel - \frac{GM_E\rho_\alpha}{R^2}\mathbf{r}_\parallel \tag{7}$$

$$\rho_\alpha\frac{dV_{\perp\alpha}}{dt} = en_\alpha\left(\frac{V_\alpha\times B}{c} - \sum_i\frac{n_i}{n_e}\frac{V_i\times B}{c}\right) + \frac{n_\alpha}{n_e}\left(\frac{J\times B}{c} - (\nabla P_e)_\perp\right) - (\nabla P_\alpha)_\perp - \frac{GM_E\rho_\alpha}{R^2}\mathbf{r}_\perp \tag{8}$$

where the $\parallel$ and $\perp$ subscripts indicate components parallel and perpendicular to the magnetic field, respectively. To remove high-frequency cyclotron oscillations, the different ion species are assumed to have the same drifts across the field line, i.e.,

$$\mathbf{V}_\perp = \frac{\sum_i \rho_i\mathbf{V}_{i,\perp}}{\sum_i\rho_i}. \tag{9}$$

This approximation is the same as assumed in MHD, and is equivalent to assuming that the convective drifts are much larger than the gradient B drifts. For the calculated bulk temperatures (<10 keV), this assumption is true for the majority of the plasma, but the particles in the tail of the distribution can have significant gradient B drifts particularly in the inner magnetosphere. Such drifts are not included in the present model. Assuming (9) the velocity of the perpendicular ion flow is given by

$$\sum_\alpha\rho_\alpha\frac{dV_{\perp\alpha}}{dt} = \left(\frac{J\times B}{c} - (\nabla P_e)_\perp\right) - \sum_\alpha(\nabla P_\alpha)_\perp - \sum_\alpha\frac{GM_E\rho_\alpha}{R^2}\mathbf{r}_\perp \tag{10}$$

where

$$\frac{\partial P_\alpha}{\partial t} = -\gamma\nabla(P_\alpha\mathbf{V}_\alpha) + (\gamma-1)\mathbf{V}_\alpha\nabla P_\alpha \tag{11}$$

The above equations are solved using a two-step Lax-Wendroff differencing scheme (Richtmyer and Morton, 1967) with Lapidus smoothing on plasma properties only (Sod, 1978). The latter is required to remove unphysical grid point oscillations across sharp discontinuities such as the bow shock. The equations are solved on a structured cartesian grid The grid spacing then increases as one moves outward, from 0.4 R_E in the dayside and mid-tail regions, to about 3 R_E in the distant tail at $x\simeq -200R_E$ (GSM) and at the flanks at $\pm 60R_E$. The solar wind boundary is at $x = 35$ R_E.

The inner radius of the simulations is set to 3 R_E which is typical of global simulation models. However, at 3 R_E the effective gravitational force on oxygen would be negligible. Therefore in order to ensure that the oxygen ions experience essentially the same average gravitational force within 1 to 2 R_E of the inner boundary, the gravity term $g = GM_E/R_E^2$ in the above equations is set at 30 m/s^2 as opposed to its actual value of 10 m/s^2. At higher altitudes convective or centrifugal processes dominate any effects that the enhanced gravitation field might have on the outflowing ions. Test runs with this value show that the outflow of oxygen is inhibited relative to the H^+ outflow when there is only weak forcing by the solar wind.

A dipole magnetic field is imposed on the grid with its field strength equivalent to the terrestrial magnetic field. A plasma with a density of 400 cm^{-3} is placed around the inner radius. This high density plasma represents the plasmaspheric/ionospheric source and is similar to observed densities (e.g., Harris et al., 1970; Parks, 1991). The initial profile is assumed to decrease as R^{-6}. When ionospheric oxygen is assumed to be present it is given the same density profile with a relative concentration of 10%. Due to the interaction with the solar wind the plasma and magnetic field profile can and is strongly distorted from this initial profile. For simplicity the boundary density is held fixed.

The initial plasma temperature in the equatorial region is assumed to decrease as R^{-3}. The initial pressure along each flux tube is assumed constant (i.e., set by mapping the simulation grid point along the dipole field line to the equator). The equatorial bulk temperature is set to about 60 eV and in the polar cap it is less that 0.3 eV. The high temperature at the equator allows for the presence of some ring current/plasma sheet population (e.g., 400 cm^{-3} and 3 eV plasmaspheric plasma mixed with a 0.5 cm^{-3} and 40 keV ring current/plasma sheet population) for an energy density of 20 keV/cm^3 (cf. Parks, 1991). The latter population may be fractionally on the high side, but certainly within the observed range. The low temperature in the polar cap region is also within the observed range and limits thermal outflow of ionospheric plasma. The total ion outflow seen in the simulations is about 6×10^{26} ions/s for the northward IMF case increasing to 2×10^{27} ions/s for the southward IMF. These numbers are of the order of those estimated by Chappell et al. (1987) and more recent updates by Yau and André

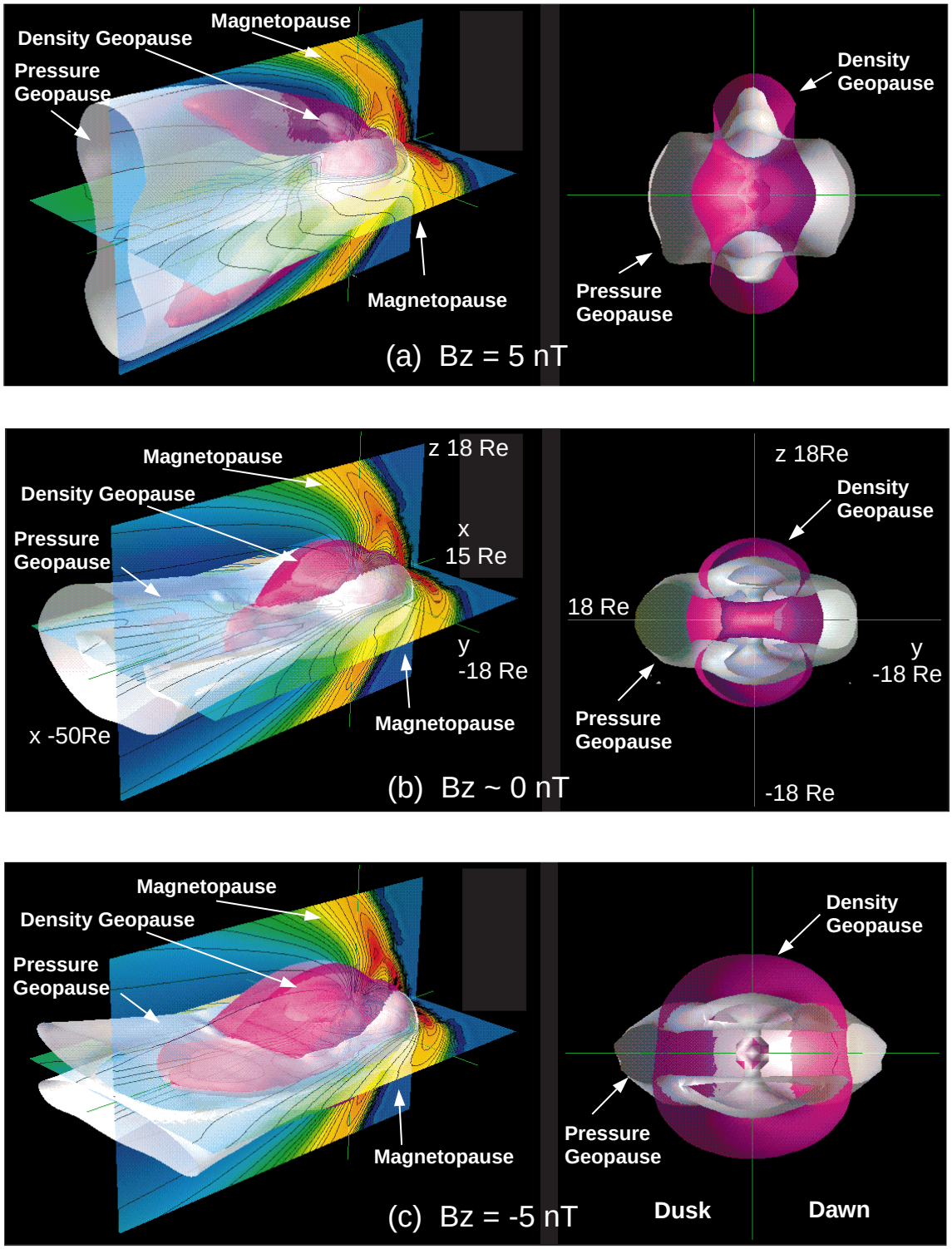

Fig. 1. The position of the density and pressure geopauses as viewed from the dawnside (left-hand side) and from the tail cut at $x = -15R_E$ (right-hand side). Contours of the plasma pressure in the noon–midnight meridian and equatorial planes are given on the left-hand side to provide an indication of the relative position of the magnetopause. The density geopause is seen to expand as IMF B_z becomes increasingly more southward. The pressure geopause is larger than the density geopause, which indicates that ionosphere is providing significant amounts of hot plasma to the central plasma sheet.

(1997). The introduction of gravity reduces this outflow only fractionally (see Section 3) for the H^+ ions but does limit the oxygen outflow as noted earlier. Decreasing (increasing) the outflow by reducing the temperature or density at the inner boundary will decrease (increase) the size of the geopause seen in the following results.

The system is initially driven by a solar wind with a constant density of 6 cm^{-3} and a speed of 400 km/s for a solar wind dynamic pressure of about 2 nPa. The simulations are first run for 2-h real time to attain an approximate equilibrium for the magnetosphere. The IMF during this initialization period is set at $\mathbf{B} = (-1.25, 0, 1.25)$ nT. The inclusion of IMF B_x is not important in the present case, but does allow the leakage of magnetospheric plasma in the upstream regions when the normal component of the IMF vanishes. After this initialization, IMF B_z is ramped down over a period of one hour to -1.25 nT. Since the average B_z is zero for this period these results will be referred to as the weak average IMF case. The IMF B_z is then made very southward at -5 nT for one hour and the results are then compared with those attained when the IMF is instead made northward to 5 nT for 1 h (see Section 3). The one-hour period has been chosen because at least up the midtail region it is sufficient for the magnetosphere to reach an approximate equilibrium that is approximately independent of the IMF history. A one hour time scale is also typical of IMF conditions seen in the solar wind. In the distant tail, the time period is not sufficient and its configuration is dependent on the IMF history. In order to illustrate some of these transients and their effects on the magnetosphere, particularly for substorm conditions, results are presented in Section 4 when the northward IMF occurs directly after a period of sustained southward IMF.

3. Steady state response

The concept of the geopause as proposed by Moore (1991) is important as it provides a ready means to visualize the different areas of magnetosphere and the supplying of plasma from either the ionosphere or solar wind. Within the density geopause, the ionosphere primarily provides the plasma while outside the geopause solar wind is the dominant source of plasma. However, as noted by Winglee (1998a, 1998b), there is a second physically important geopause called the pressure geopause which is useful in identifying the pressure sources needed to support key structures such as the tail current sheet and the low latitude boundary layer (LLBL). Differences in the location between the density and pressure geopauses can provide insight into which of the two sources is providing the hot plasma and which is providing the cold plasma.

As an example, the left-hand side of Fig. 1 shows the positions of the density and pressure geopauses in relation to magnetopause for simulations without oxygen or gravity included. The magnetosheath can be identified from the pressure contours shown as cuts in the noon–midnight meridian and equatorial plane and is seen as a region of high pressure (indicated by the red and orange contours). The magnetopause is just inside the high-pressure region and it is in general much larger than the density geopause, which is shown as the magenta surface, and the pressure geopause, which is shown as the gray surface. The right-hand side shows cross-tail views of the density and pressure geopauses taken at $x = -15R_E$.

For northward IMF, the density geopause is limited to the lobes and the plasmasphere, so that most of the density in the plasma sheet is provided by the solar wind. On the other hand, the pressure geopause is seen to encompass the density geopause and have a larger extent down the tail although it remains restricted to a few R_E in width (y). This difference in location between the density and pressure geopauses means that in this region of the tail it is the ionospheric source which is providing the bulk of the hot plasma but it is the solar wind source which is providing the bulk of the density.

The dominance of the solar wind source in populating the magnetosphere for northward IMF is produced by high-latitude reconnection that allows magnetosheath plasma to become attached to closed-field lines. Subsequent convection of these field lines enables this magnetosheath plasma to appear deep within the magnetosphere. This plasma does not undergo as strong a compression and adiabatic heating as the ionospheric plasma from the lobe/plasma sheet boundary. As a result, it is the ionosphere that provides the hot plasma in the mid-regions of the plasma sheet even though the density is primarily of solar wind origin.

As the IMF is reduced to zero (Fig. 1(b)), stronger convection of the ionospheric plasma into the plasma sheet is seen so that the density geopause folds down onto the plasma sheet, i.e. ionosphere starts to play a greater role in populating the plasma sheet with density. At the same time the pressure geopause and hence the hot plasma region are seen to expand in width across the tail. This expansion in y continues as the IMF becomes southward (Fig. 1(c)).

The change in the configuration of the geopause as the IMF becomes southward can be understood as follows. First, high-latitude reconnection is replaced by dayside reconnection. For reconnection near the subsolar region the newly reconnected field-lines are convected over the polar cap and into the nightside and into the mantle. These fields lines are mass loaded with

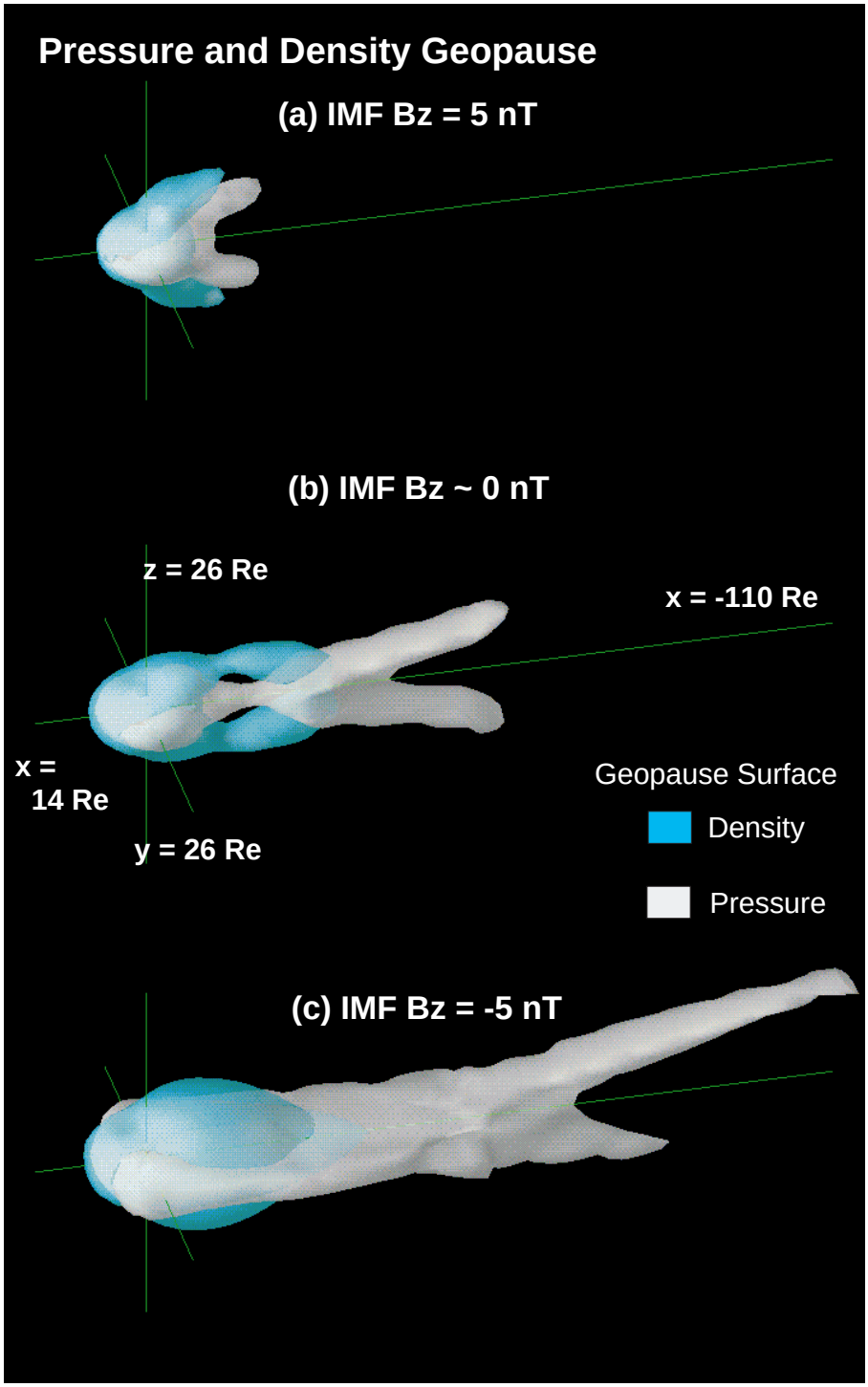

Fig. 2. Changes in the density and pressure geopauses when gravity and O^+ are included. The scale size along the x-axis is twice as large as in Fig. 1. There is some shrinkage of the geopauses, most notably for northward IMF, under the influence of gravity.

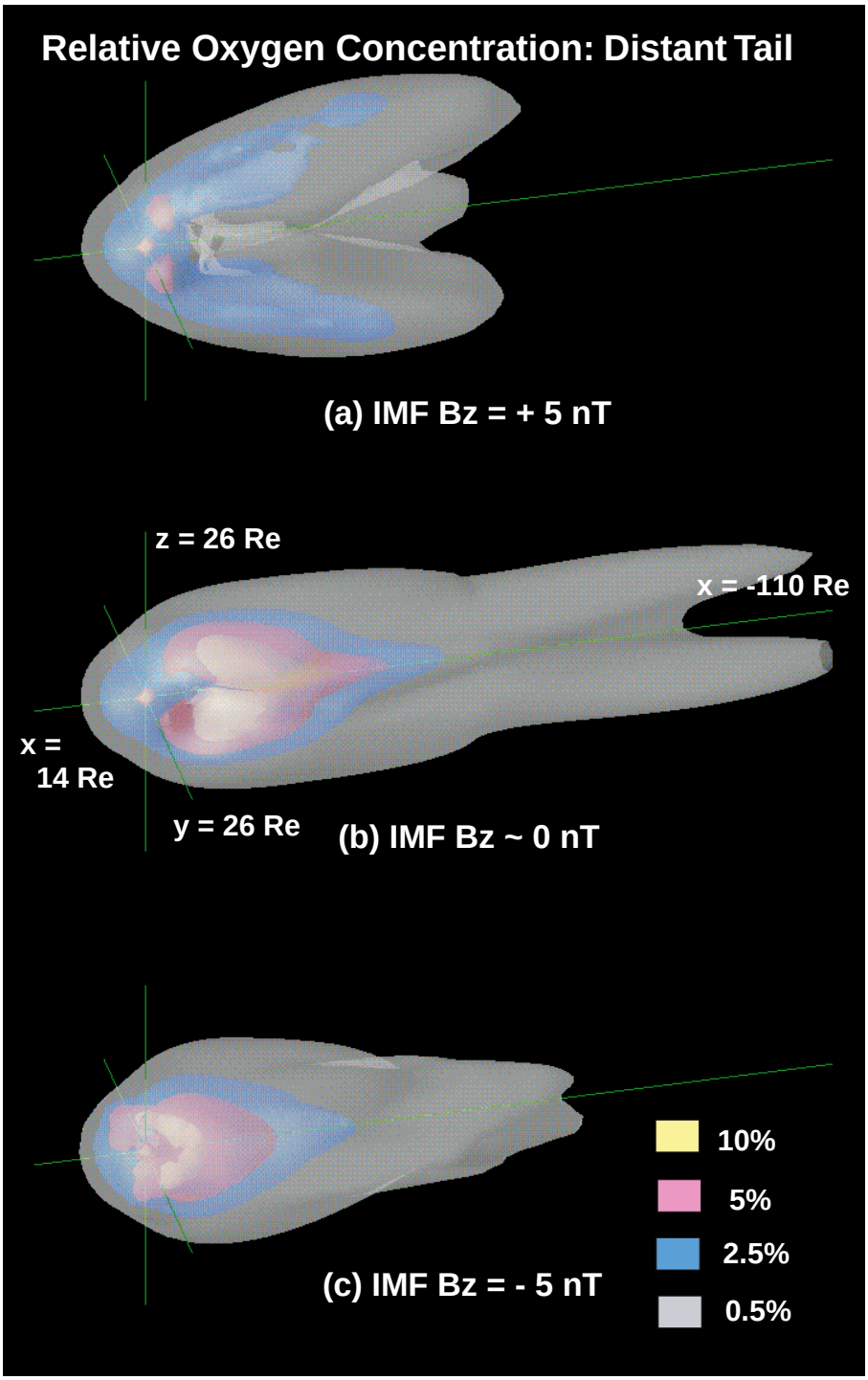

Fig. 3. Isosurfaces of the oxygen concentration corresponding to Fig. 2. These isosurfaces have similar shapes to the density geopauses in Fig. 2. Very little oxygen is able to escape the ionosphere for northward IMF and while enhance outflows are generated for southward IMF most of the oxygen is confined to the inner magnetosphere, and it is the weak average IMF configuration that leads to the deepest penetration of oxygen into the deep tail.

solar wind plasma but the speed of the plasma means that much of the plasma is convected down the tail before it has a chance to enter the current sheet. This is seen in the model as a lowering of the height of the density geopause beyond about 15 R_E. Field lines that reconnect on the flanks are convected around the side and lead to the solar wind source for the most part along the Sun–Earth line providing the plasma for the low latitude boundary layer. Since convection in the tail is predominantly along the Sun–Earth line, this plasma only has limited access to the middle of the current sheet. At the same time the enhanced polar cap potential means that more centrifugal acceleration of ionospheric plasma can occur and it is for this reason that the ionospheric source starts to play an increasingly important role in the dynamics of the mid-tail region as seen by the expansion of the geopause both down the tail and across in width.

The changes in the positions of the density and pressure geopauses with the introduction of gravity and oxygen are shown in Fig. 2. Note that the scale size is twice as long so that the deep tail dynamics can also be seen. While the shapes of the geopauses are qualitatively similar to that in Fig. 1, the introduction of gravity causes the geopauses to slightly contract inwards for northward IMF (Fig. 2(a)) and to a lesser extent in Fig. 2(b). However, for southward IMF, the ionospheric outflows are not noticeably impeded by the introduction of gravity.

Gravity has the weakest effect for southward IMF because the outflows in the model are primarily driven by centrifugal acceleration as described by Horwitz (1987). Much like a bead on a rotating wire, plasma at high latitudes experienced a centrifugal acceleration as the field lines are convected over the polar cap. Since the cross-polar cap potential and hence the convection speed are largest for southward IMF, the outflows attain the highest velocities for southward IMF. The centrifugal acceleration of H^+ is such that it easily overcomes the gravitational barrier for southward IMF and marginally so for northward IMF.

The corresponding relative concentrations of oxygen are shown in Fig. 3. For northward IMF, the oxygen distribution has a similar shape to the density geopause in that most of the density is concentrated in the lobes and plasmasphere. However, the relative concentration is very weak with the plasmasphere attaining 2.5% oxygen and with the central lobes attaining only about 0.5% at 50 R_E and substantially less deep into the tail. These concentrations are obtained for ionospheric boundary conditions at 10%. These low concentrations in magnetosphere arise because the bulk of the oxygen cannot overcome the gravitational potential and some additional acceleration is needed.

For weak average IMF (see Fig. 3(b)), substantial increases in the relative oxygen concentration can be seen even down into the deep tail. The model values of 0.5% are of order of the average 1% concentration reported by Seki et al. (1998). In the mid-tail region, concentrations of 5–10% can be seen.

Paradoxically for strong southward IMF, the oxygen is unable to escape into the deep tail as seen by the contraction of the isosurfaces in Fig. 3(c). The apparent shrinkage is due to the fact that the enhanced convection electric field causes the oxygen to convect into the plasma sheet within the inner- to mid-tail region of the plasma sheet. The enhanced convective electric field then causes the oxygen to convect into the dayside so that strong sustained southward IMF can lead to enhance dayside oxygen concentrations of 5–10%, as seen in Fig. 3(c), but relatively little concentration in the deep tail. Thus, for these steady-state conditions, the dayside magnetosphere acts as a reservoir for heavy ionospheric ion species.

4. Transient effects

If one were to average the oxygen seen in the three cases in Fig. 3 then the average concentration would be smaller than the observations of Seki et al. (1998). There are two possible sources for this discrepancy. The first is that the model does not take into account changes in the relative concentration of oxygen at low altitudes. While this variation is known to occur, a direct relationship with solar wind conditions is not known at this time and therefore cannot be incorporated into the model. The second factor, which is at least equally important, is that transients can lead to the ejection of the oxygen rich plasma in the inner magnetosphere into the deep tail.

As an example, Fig. 4 shows the evolution of the density and pressure geopauses for a northward turning of the IMF to 5 nT following the 1-h period of southward (−5 nT) IMF of Fig. 2(c). As already noted, during this period of southward IMF there is a buildup of plasma in the inner magnetosphere. It takes approximately 15 min for this northward IMF turning to reach the terminator. Thus the geopauses in Fig. 4(a) are still approximately the same as that in Fig. 2(c). However, with the arrival of the northward IMF, the cross-polar cap potential decreases but the inner magnetosphere still has substantial amounts of plasma from the previous period southward IMF. As a result there is a plasma excess that has to be lost. It can be lost either through the precipitation of particles into ionosphere or the ejection of plasma down the tail. The latter can be seen in Fig. 4(b) as enhanced concentration of ionospheric plasma moving into the mid-tail region, and is actually associated with the ejection of a plasmoid, which is not shown.

In the model, this flow of ejected plasma has signifi-

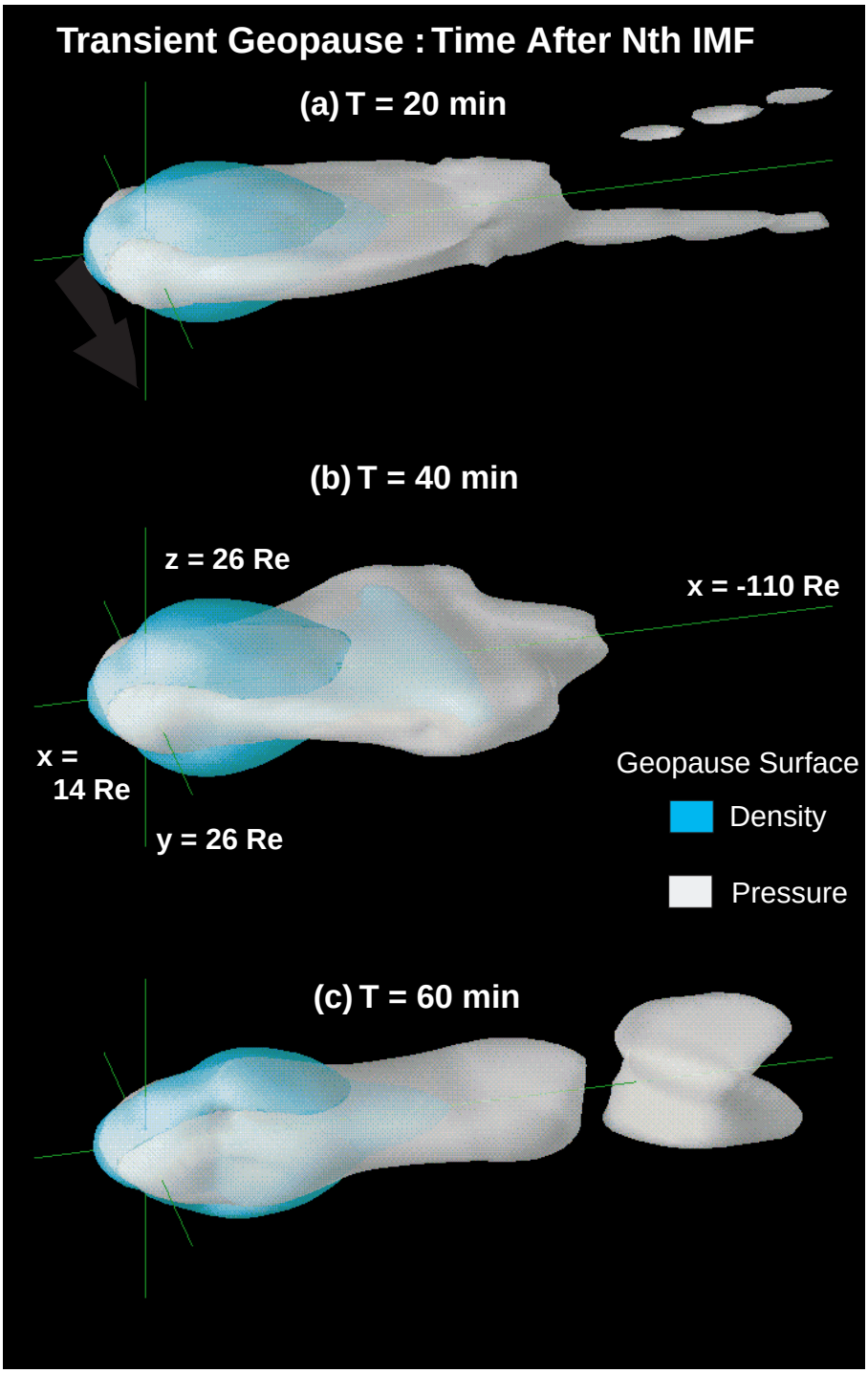

Fig. 4. Changes in the positions of the geopauses following a northward (5 nT) turning of the IMF that follows the one hour southward (−5 nT) IMF shown in Fig. 2(c). The times given are from the start of the turning and it takes approximately 15 min for it to propagate from the solar wind boundary to the terminator. The northward turning leads to the ejection of plasma enriched in ionospheric ions into the deep tail.

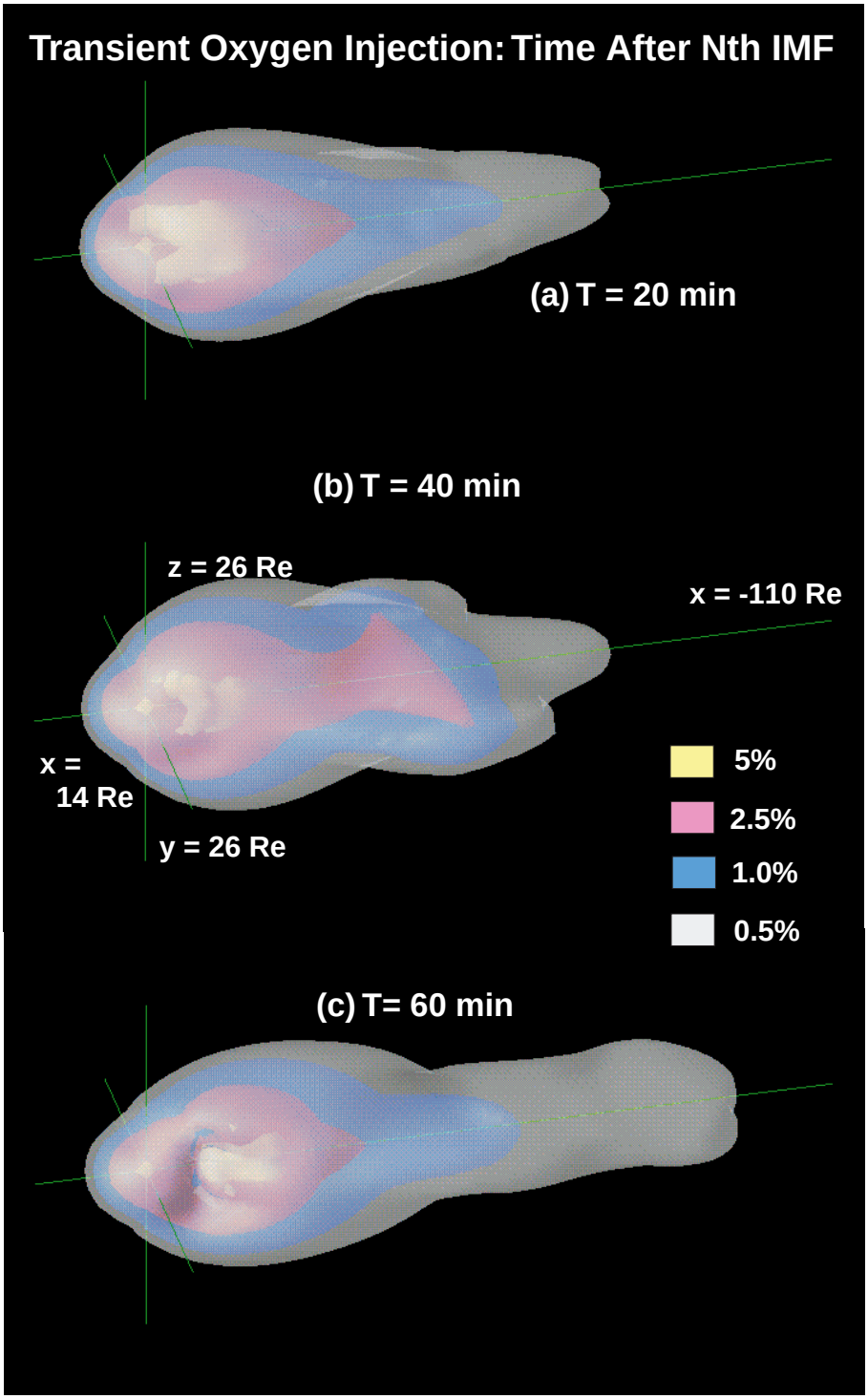

Fig. 5. The relative concentration of oxygen corresponding to Fig. 4. The northward turning leads to enrichments in O^+ into the mid- to deep tail. The O^+ concentrations appear higher than the steady-state configurations in Fig. 3. The average concentration in the tail is of order of 1%, comparable to the Geotail observations reported by Seki et al. (1998).

cant structure. The leading edge is seen to have high concentration of solar wind plasma while the trailing edge contains an ionospheric-rich component as seen in Fig. 4(b). As the ejected plasma moves into the deep tail, there is some dispersion of the plasma so that most of the density is of solar wind origin. Nevertheless a hot ionospheric component is still present, as seen by the isolated geopause surface in Fig. 4(c).

With the ejection of this ionospheric component, the density and pressure geopauses in the near-Earth region shrink in width, and begin to approach the shape seen in Fig. 2(b). However, about another 20 min is required before they approach the shape of the near steady-state condition of Fig. 2(a). Thus, solar wind transients can lead to substantial deformations of the geopauses and the apparent time scale for near steady-state conditions to be attained appears to be of the order of an hour.

The corresponding changes in oxygen concentration are shown in Fig. 5. It is seen that the ejection of ionospheric plasma down the tail is also clearly evident in the oxygen profile. Thus the presence of enhanced O^+ can serve as an important marker for the geopause. Even for ionospheric boundary conditions fixed at 10%, concentrations of oxygen can reach as high as 2.5% in the mid-tail region. Higher concentrations would be expected if the ionospheric boundary condition were correspondingly increased.

The corresponding average concentration over the full period is about 0.5% in the distant tail at several tens of R_e. This value is comparable to that observed by Seki et al. (1998). This agreement would suggest that the geopauses derived in the model are semi-quantitatively correct. Furthermore the geopauses derived in the model are driven by ionospheric outflows that are consistent with those inferred from polar orbiting spacecraft (Chappell et al., 1987). In other words the model can account for the presence of oxygen in the deep tail without requiring extreme conditions and it is natural for the ionosphere to play an important role in producing significant portions of the plasma in the magnetosphere.

5. Summary and conclusions

In this paper, results are presented from the first global multi-fluid simulation of the magnetosphere that includes multiple ion species. Such modeling is the only means for identifying the relative contributions of the ionospheric and solar wind sources over the whole magnetosphere and for determining the build up of different ion species within it. This problem is important for the dynamics of the magnetosphere since the presence of hot and cold plasma and/or the presence of light and heavy ion species can substantially change the response of the magnetosphere to changes in solar wind conditions. In addition these different plasma components or ion species can be used as key diagnostics for the entry and transport of plasma and its energization within the magnetosphere.

To visualize the origins of the different plasma sources within the magnetosphere, we utilize the concepts of the density and pressure geopauses that mark the boundaries where the ionospheric and solar wind sources provide equal contributions to the plasma density and pressure, respectively. For the northward IMF, the density geopause is restricted to the plasmasphere and lobes. The relatively strong entry of solar wind plasma into the magnetosphere is facilitated in this case by high-latitude reconnection and subsequent convection of the newly reconnected field lines into the magnetosphere. On the other hand, the pressure geopause extends beyond the density geopause, into the plasma sheet but remains very restricted in width. This difference between the density and pressure geopauses is indicative of the ionospheric plasma being strongly heated by adiabatic compression as it is convected into the plasma sheet, so that in the vicinity of the noon–midnight meridian the ionosphere is the dominant source of hot plasma. As the IMF becomes increasingly southward, the density and pressure geopauses are seen to encompass the plasma sheet and move down the tail as well as across the tail.

In the model the oxygen outflows are driven by centrifugal acceleration arising from convection of the field lines over the polar cap. Propagation of ionospheric oxygen into the magnetosphere is dependent on this acceleration plus the strength of the convective electric field in the tail. For sustained northward IMF, the convection speed is relatively low and the centrifugal acceleration is insufficient to overcome the gravitational potential well so that oxygen outflows are very weak and primarily restricted to the plasmasphere and lobes.

For sustained southward IMF, the fast polar cap flows (or equivalently the enhanced cross-polar cap potential) are able to drive stronger oxygen outflows. However the enhanced convective electric field causes this oxygen to be convected into the plasma sheet and around to the dayside. As a consequence even for these enhanced oxygen outflows, oxygen only has limited access to the deep tail. Paradoxically for steady state conditions, deep tail oxygen is most likely to be observed for weak average IMF where there is a balance between centrifugal acceleration and convection into the plasma sheet.

The situation is very much more different if transients in the solar wind are considered. For example during a period which includes 1 h of sustained southward IMF followed by 1 h of sustained northward (such that might be associated with substorms), the

period of southward IMF (i.e., growth phase) leads to an enhanced loading of oxygen in the inner magnetosphere. With the northward turning of the IMF, ionospheric plasma including oxygen is ejected tailward and leads to oxygen concentrations in the deep tail much larger than seen in the steady-state simulations. The trailing edge of the ejected plasma associated with substorms activity shows the strongest concentrations of ionospheric ions while the leading edge is primarily of solar wind origin.

The corresponding oxygen concentrations observed in the deep tail under these conditions are consistent with the observations of Seki et al. (1998). This result is not only important in itself, but it suggests that the density and pressure geopauses derived from the present simulations are approximately the right order of magnitude. This means that the ionospheric source can be the important source of plasma to magnetosphere, particularly during disturbed times, as suggested by Chappell et al. (1987).

This is not to say that solar wind source is not an important source of plasma to the magnetosphere. For northward IMF it is the solar wind source that dominates the magnetosphere, and the model can account for the high correlation, particularly for northward IMF, between the solar wind and plasma sheet densities (Terasawa et al., 1997; Borovsky et al., 1997). Strong mixing of the two plasmas driven by reconnection and convection is expected during periods of variable solar wind conditions. This means that components from the two different sources should be expected to be seen throughout much of the magnetosphere, albeit at highly varying concentrations.

Acknowledgements

This work was supported by NSF Grant ATM-9731951 and by NASA grants NAG5-6244, NAG5-8089 to the Univ. of Washington. The simulations were supported by the Cray T-90 at the San Diego Supercomputing Center which is supported by NSF.

References

André, Yau, A., 1997. Theories and observations of ion energization and outflow in the high latitude magnetosphere. Space Sci. Rev. 80, 27.

Borovsky, J.E., Thomsen, M.F., McComas, D.J., 1997. The superdense plasma sheet: plasmaspheric origin, solar wind origin, or ionospheric origin? J. Geophys. Res 97, 22089.

Chang, T., Crew, G.B., Hershkowitz, N., Jasperse, J.R., Retterer, J.M., Winningham, J.D., 1986. Geophys. Res. Lett 13, 636.

Chappell, C.R., Moore, T.E., Waite Jr., J.H., 1987. The ionosphere as a fully adequate source of the earth's magnetosphere. J. Geophys. Res 92, 5896.

Cladis, J.B., 1986. Parallel acceleration and transport of ions from polar ionosphere to plasma sheet. Geophys. Res. Lett 13, 893.

Collin, H.K., Peterson, W.K., Shelley, E.G., 1987. Solar cycle variation of some mass dependent characteristics of upflowing beams of terrestrial ions. J. Geophys. Res 92, 4757.

Delcourt, D.C., Chappell, C.R., Moore, T.E., Waite Jr., J.H., 1989. A three-dimensional numerical model of ionospheric plasma in the magnetosphere. J. Geophys. Res 94, 11893.

Delcourt, D.C., Sauvaud, J.A., Moore, T.E., 1993. Polar wind ion dynamics in the magnetotail. J. Geophys. Res 98, 9155.

Fujimoto, M., Terasawa, T., Mukai, T., 1998a. Structure of the low-latitude boundary layer: a case study with Geotail data. J. Geophys. Res 103, 2297.

Fujimoto, M., Terasawa, T., Mukai, T., 1998b. Plasma entry from the flanks of the near-earth magnetopause: Geotail observations. J. Geophys. Res 103, 4391.

Ghielmetti, A.G., Johnson, R.G., Sharp, R.D., Shelley, E.G., 1978. The latitudinal, diurnal, and altitudinal distributions of upflowing energetic ions of ionospheric origin. Geophys. Res. Lett 5, 59.

Gorney, D.J., Clarke, A., Croley, D., Fennell, J.F., Luhmann, J., Mizera, P., 1981. The distribution of ion beams and conics below 8000 km. J. Geophys. Res 86, 83.

Harris, K.K., Sharp, G.W., Chappell, C.R., 1970. Observations of the plasmapause from OGO 5. J. Geophys. Res 75, 219.

Hirahara, M., Mukai, T., Terasawa, T., Machida, S., Saito, Y., Yamamoto, T., Kokubun, S., 1996. Cold dense ion flows with multiple components observed in the distant tail lobe by Geotail. J. Geophys. Res 101, 7769.

Klumpar, D.M., 1979. Tranversely accelerated ions: an ionospheric source of hot magnetosphericthe ions. J. Geophys. Res 84, 4229.

Horwitz, J.L., 1987. Core plasma in the magnetosphere. Rev. Geophys. Spc. Phys 25, 579.

Lennartsson, W., 1987. Plasma sheet ion composition at various levels of geomagnetic and solar activity. Physica Scripta 36, 367–371.

Lennartsson, W., 1992. A scenario for solar wind penetration of Earth's magnetic tail based on ion composition data from the ISEE 1 spacecraft. J. Geophys. Res 97, 19221.

Li, Q., Winglee, R.M., Wilber, M., Chen, L., Parks, G., 1999. The geopause in relation to the plasma sheet and the low latitude boundary layer: comparison between wind observations and multi-fluid simulations. J. Geophys. Res., in press.

Moore, T.E., Lockwood, M., Waite Jr., J.H., Chandler, M.O., Peterson, W.K., Wiemer, D., Sugiura, M., 1986. Upwelling O^+ source characteristics. J. Geophys. Res 91, 7019.

Moore, T.E., 1991. Origins of magnetospheric plasma. Rev. Geophys 29, 1039.

Moore, T.E., Delcourt, D.C., 1995. The Geopause. Rev. Geophys 33, 175.

Parks, G.K., 1991. Physics of Space Plasmas. Addison-Wesley, Redwood City, CA.

Pollock, C.J., et al., 1990. A survey of upwelling ion event characteristics. J. Geophys. Res 95, 18969.

Richtmyer, R.D., Morton, K.W., 1967. Difference Methods for Initial Value Problems. Interscience, New York, p. 300.

Roberts, W.T., et al., 1987. Heavy ion density enhancements in the outer plasmasphere. J. Geophys. Res 92, 13499.

Seki, K., Hirahara, M., Terasawa, T., Shinohara, I., Mukai, T., Saito, Y., Machida, S., Yamamoto, T., Kokubun, S., 1996. Coexistence of Earth-origin O^+ and solar wind-origin H^+/He^{++} in the distant magnetotail. Geophys. Res. Lett 23, 985.

Seki, K., Hirahara, M., Terasawa, T., Mukai, T., Saito, Y., Machida, S., Yamamoto, T., Kokubun, S., 1998. Statistical properties and possible supply mechanisms of tailward cold O^+ beams in the lobe/mantle regions. J. Geophys. Res 103, 4477.

Sharp, R.D., Johnson, R.G., Shelley, E.G., 1977. Observations of an ionospheric acceleration mechanism producing energetic (keV) ions normal to the geomagnetic field direction. J. Geophys. Res 82, 3324.

Shelley, E.G., Johnson, R.G., Sharp, R.D., 1972. Satellite observations of an Ionospheric acceleration mechanism. J. Geophys. Res 77, 6104.

Singh, N., Schunk, R.W., 1985. A possible for the observed streaming of O^+ and H^+ ions that nearly equal speeds in the distant magnetotail. J. Geophys. Res 90, 6361.

Sod, G.A., 1978. A survey of several finite difference methods for systems of nonlinear hyperbolic conservation laws. J. Computational Phys 27, 1.

Su, Y.-J., Horwitz, J.L., Wilson, G.R., Richards, P.G., Brown, D.G., Ho, C.W., 1998. Self-consistent simulation of the photoelectrons-driven polar wind from 120 km to 9 R_E, altitude. J. Geophys. Res 103, 2279.

Terasawa, T., Fujimoto, M., Mukai, T., Shinohara, I., Saito, Y., Yamamoto, T., Machida, S., Kokubun, S., Lazarus, A.J., Steinberg, J.T., Lepping, R.P., 1997. Solar wind control of density and temperature in the near-Earth plasma sheet: WIND/GEOTAIL collaboration. Geophys. Res. Lett 24, 935.

Waite Jr., J.H., 1985. Escape of suprathermal O^+ ions in the polar cap. J. Geophys. Res 90, 1619.

Winglee, R.M., 1998a. Multi-fluid simulations of the magnetosphere: the identification of the geopause and its variation with IMF. Geophys. Res. Lett 25, 4441.

Winglee, R.M., 1998b. Imaging the ionospheric and solar wind sources in the magnetosphere through multi-fluid global simulations. Physics of Space Plasmas 15, 345.

Winglee, R.M., Dusenbery, P.B., Collin, H.L., Lin, C.S., Persoon, A.M., 1989. Simulations and observations of heating auroral ion beams. J. Geophys. Res 94, 8943.

Yau, A.W., André, M., 1997. Source of ion outflow in the high latitude ionosphere. Space Sci. Rev 80, 1.

Yau, A.W., Beckwith, P.H., Peterson, W.K., Shelley, E.G., 1985. Long-term (solar cycle) and seasonal variations of upflowing ionospheric ion events at DE 1 altitudes. J. Geophys. Res 90, 6395.

Yau, A.W., Peterson, W.K., Shelley, E.G., 1988. Quantititive parameterization of energetic ionospheric outflow. In: Modeling Magnetospheric Plasma, Geophysical Monograph, 44. American Geophysical Union, Washington, DC, p. 211.

Yau, A.W., Whalen, B.A., Goodenough, C., Sagawa, E., Mukai, T., 1993. EXOSD (Akebono) observations of molecular NO^+ and N_2^+ upflowing ions in the high latitude auroral ionosphere. Geophys. Res. Lett 18, 345.